AFRL-RV-PS-
TP-2015-0003

TEMPERATURE DEPENDENCES FOR THE REACTIONS OF O_2^- and O^- WITH N AND O ATOMS IN A SELECTED-ION FLOW TUBE INSTRUMENT

Shaun G. Ard, et al.

07 January 2015

Journal Article

AIR FORCE RESEARCH LABORATORY
Space Vehicles Directorate
3550 Aberdeen Ave SE
AIR FORCE MATERIEL COMMAND
KIRTLAND AIR FORCE BASE, NM 87117-5776

REPORT DOCUMENTATION PAGE

Form Approved
OMB No. 0704-0188

1. REPORT DATE *(DD-MM-YYYY)*	**2. REPORT TYPE**	**3. DATES COVERED** *(From - To)*
07-01-2015	Journal Article	01 May 2013 - 02 Aug 2013

4. TITLE AND SUBTITLE

Temperature dependences for the reactions of O_2^- and O^- with N and O atoms in a selected-ion flow tube instrument

5a. CONTRACT NUMBER

5b. GRANT NUMBER

5c. PROGRAM ELEMENT NUMBER
61102F

6. AUTHOR(S)
Shaun G. Ard, Joshua J. Melko, Bin Jiang[1], Yongle Li[1], Nicholas S. Shuman, Hua Guo[1], and Albert A. Viggiano

5d. PROJECT NUMBER
2303

5e. TASK NUMBER
PPM00004294

5f. WORK UNIT NUMBER
EF002012

7. PERFORMING ORGANIZATION NAME(S) AND ADDRESS(ES)
Air Force Research Laboratory
Space Vehicles Directorate
3550 Aberdeen Avenue SE
Kirtland AFB, NM 87117-5776

[1]Department of Chemistry and Biology
University of New Mexico
Albuquerque, NM 87131

8. PERFORMING ORGANIZATION REPORT NUMBER
AFRL-RV-PS-TP-2015-0003

9. SPONSORING / MONITORING AGENCY NAME(S) AND ADDRESS(ES)

10. SPONSOR/MONITOR'S ACRONYM(S)
AFRL/RVBXT

11. SPONSOR/MONITOR'S REPORT NUMBER(S)

12. DISTRIBUTION / AVAILABILITY STATEMENT

Approved for public release; distribution is unlimited. (377ABW-2013-0465 dtd 04 Jun 2013)

13. SUPPLEMENTARY NOTES

The Journal of Chemical Physics: 21 October 2014. Government Purpose Rights.

14. ABSTRACT

Rate constants for the reactions of $O2^-$ and O^- with N and O atoms have been measured for the first time as a function of temperature from 173 to 500 K for O^- reactions and 173 to 400 K for $O2^-$ reactions. Room temperature rate constants for $O2^-$ reacting with N and O are 3.1×10^{-10} and 1.7×10^{-10} $cm^3\ s^{-1}$, respectively, and the corresponding O^- rate constants are 1.7×10^{-10} and 1.5×10^{-10} $cm^3\ s^{-1}$, in good agreement with previous values. Temperature dependences are about $T^{-1.7}$ for both $O2^-$ reactions and $T^{-0.6}$ and $T^{-1.3}$ for the reactions of O^- with N and O, respectively. Branching for the $O2^-$ reaction with N is found to predominantly form O^- (>85%) in contrast to previous measurements, which reported $NO2 + e^-$ as the main channel. Calculations point to the present results being correct. The potential energy surface for this reaction was calculated using density functional theory, coupled cluster with singles, doubles (triples), complete active space self-consistent field, and complete active space second-order perturbation methods and is found to be quite complex, with agreement between the calculated surface and the observed kinetic data only possible through the inclusion of dynamical correlation.

15. SUBJECT TERMS

Physical Chemistry, Atomic and Molecular Chemistry, Reaction rate constants, Atom reactions, ion molecule reactions, heavy ion reactions, chemical reactions

16. SECURITY CLASSIFICATION OF:			**17. LIMITATION OF ABSTRACT**	**18. NUMBER OF PAGES**	**19a. NAME OF RESPONSIBLE PERSON**
a. REPORT	**b. ABSTRACT**	**c. THIS PAGE**			Dr. Albert Viggiano
Unclassified	Unclassified	Unclassified	Unlimited	10	**19b. TELEPHONE NUMBER** *(include area code)*

Temperature dependences for the reactions of O_2^- and O^- with N and O atoms in a selected-ion flow tube instrument

Shaun G. Ard,[1] Joshua J. Melko,[1] Bin Jiang,[2] Yongle Li,[2] Nicholas S. Shuman,[1] Hua Guo,[2] and Albert A. Viggiano[1,a)]
[1]*Air Force Research Laboratory, Space Vehicles Directorate, Kirtland AFB, New Mexico 87117-5776, USA*
[2]*Department of Chemistry and Chemical Biology, University of New Mexico, Albuquerque, New Mexico 87131, USA*

(Received 2 August 2013; accepted 9 September 2013; published online 7 October 2013)

Rate constants for the reactions of O_2^- and O^- with N and O atoms have been measured for the first time as a function of temperature from 173 to 500 K for O^- reactions and 173 to 400 K for O_2^- reactions. Room temperature rate constants for O_2^- reacting with N and O are 3.1×10^{-10} and 1.7×10^{-10} cm^3 s^{-1}, respectively, and the corresponding O^- rate constants are 1.7×10^{-10} and 1.5×10^{-10} cm^3 s^{-1}, in good agreement with previous values. Temperature dependences are about $T^{-1.7}$ for both O_2^- reactions and $T^{-0.6}$ and $T^{-1.3}$ for the reactions of O^- with N and O, respectively. Branching for the O_2^- reaction with N is found to predominantly form O^- (>85%) in contrast to previous measurements, which reported $NO_2 + e^-$ as the main channel. Calculations point to the present results being correct. The potential energy surface for this reaction was calculated using density functional theory, coupled cluster with singles, doubles (triples), complete active space self-consistent field, and complete active space second-order perturbation methods and is found to be quite complex, with agreement between the calculated surface and the observed kinetic data only possible through the inclusion of dynamical correlation. © *2013 AIP Publishing LLC*. [http://dx.doi.org/10.1063/1.4824018]

INTRODUCTION

Already in 1961, Dalgarno suggested that O^- and O_2^- react with O atoms to detach electrons.[1] This was later confirmed by the NOAA group in 1967, who also found that N atoms detach electrons in reaction with O^- and O_2^-.[2] The potential pathways are listed in reactions (1)–(4). The NOAA group reported that reaction (1a) dominated. They further established that (2a) and (2b) competed but did not report branching ratios. These findings proved especially important for the chemistry of the D-region of the ionosphere because the reactions convert heavy ions into light e^- which impact radiowave propagation:[3–5]

$$O_2^- + N \rightarrow NO_2 + e^-, \quad \Delta_r H^\circ = -4.11\,\text{eV}, \tag{1a}$$

$$NO + O^-, \quad \Delta_r H^\circ = -2.39\,\text{eV}, \tag{1b}$$

$$O_2^- + O \rightarrow O_3 + e^-, \quad \Delta_r H^\circ = -0.66\,\text{eV}, \tag{2a}$$

$$O_2 + O^-, \quad \Delta_r H^\circ = -1.01\,\text{eV}, \tag{2b}$$

$$O^- + N \rightarrow NO + e^-, \quad \Delta_r H^\circ = -5.09\,\text{eV}, \tag{3}$$

$$O^- + O \rightarrow O_2 + e^-, \quad \Delta_r H^\circ = -3.71\,\text{eV}. \tag{4}$$

No subsequent work had been performed on reactions (1)–(4) until our group reexamined reactions (1) and (2) in 2006,[6] as part of an ongoing effort to improve on the knowledge of ionospheric chemistry.[7] In that study, we found that chemical reaction (1b) competes with detachment in the reaction of O_2^- with N. This discrepancy with the literature was attributed to using a selected ion flow tube with an external ion source rather than a flowing afterglow. Here, we refine the measurements and report the first temperature dependent measurements for all four reactions, and detail our modeling efforts for reaction (1).

EXPERIMENTAL

All experiments were performed on a selected-ion flow tube instrument that has been described in detail in Refs. 6, 8, and 9. Briefly, O_2^- was generated by associative electron attachment to O_2, while O^- was created by dissociative attachment to N_2O in a high-pressure electron impact ionization source. The ions were focused into a quadrupole mass filter, mass selected, and injected into the flow reactor via a Venturi-type inlet. Ions undergo ~10^5 collisions with helium buffer gas at pressures of 0.4 to 0.8 Torr resulting in complete or near-complete thermalization.[10] The higher pressure was used when studying the high temperature reactions because the rate constants are small and only limited amounts of atoms were formed. Higher pressure was achieved by throttling a butterfly gate valve resulting in lower pumping speeds and thus longer reaction times. Neutrals were injected 49 cm before the end of the flow tube and allowed to react with O_2^- or O^-. The

a)Author to whom correspondence should be addressed. Electronic mail: afrl.rvborgmailbox@kirtland.af.mil

product ions and residual reactant ions were sampled through a 1 mm orifice into a second quadrupole mass filter for mass analysis. A small attractive voltage (~5 V) was applied to the nose cone. Ions were detected with an electron multiplier operating in pulse counting mode. The temperature of the flow tube was varied from 173 to 500 K either by resistive heating devices or pulsed liquid nitrogen.

Nitrogen atoms were generated via microwave discharge of N_2 in a Pyrex side arm. The extent of nitrogen dissociation was small (<1%) and was varied by changing either the N_2 flow rate or the microwave discharge power. Contributions from vibrationally excited N_2 from this setup have been shown to be negligible due to collisions in the glass side arm.[11,12] Oxygen atoms were generated using a titration method that has been described in detail in Refs. 11 and 13. The surface of the glass was treated with a boric acid solution to minimize O atom losses on the walls of the cavity. NO gas was introduced at a known flow rate into the glass side arm downstream of the discharge where it quantitatively reacted with the nitrogen atoms to give ground state oxygen atoms.[11] A run started by recording ion signals with the discharge off then on without addition of NO. The decrease in the signal intensity combined with the N atom density determined the N atom rate constant. NO was then added, which converted the N into O. At low NO flows, both N and O atoms flowed into the reaction zone and the NO was completely converted to O. At higher flows, O and NO both entered the reaction zone. A change of slope occurred at the point where all N atoms were converted to O atoms, i.e., the titration end point.

RESULTS AND DISCUSSION

Figure 1 shows a set of raw data for 300 K and 0.8 Torr for the O_2^- reactions. The black triangle represents the O_2^- signal with the discharge off; the O^- signal without the discharge is near zero and is not displayed. Solid circles and squares represent discharge-on data for O_2^- and O^-, respectively. Turning the discharge on creates N atoms which decrease the O_2^- signal substantially while increasing the O^- signal due to reaction (1b). As NO was added in low concentrations, converting some of the N to O, the O_2^- signal increased indicating the O atom rate constant is smaller than the N atom rate constant with O_2^-. At NO concentrations exceeding the initial N atom concentration, the amount of O remained constant with increasing amounts of NO added. Since O_2^- does not react with NO, the signal remains constant as expected. The NO concentration at which the slope changes from positive to zero equals the initial N atom concentration, $[N]_0$. The O^- similarly increased at low NO addition but then, because O^- reacts with NO, decreased after the titration end point. The rate constant of O_2^- with N is derived from the following equation:

$$k_N = \frac{\ln \frac{[O_2^-]_{off}}{[O_2^-]_{0,on}}}{[N]_0 t}, \quad (5)$$

where the O_2^- signals are with the discharge off and on at zero NO flow and t is the reaction time. The positive slope at low NO concentrations reflects the amount that the O atom rate constant is smaller than the N atom rate constant. The O atom rate constant can be derived similarly to (5), replacing the discharge-on O_2^- signal at zero NO flow with the signal at the titration end point, where the O atom concentration equals $[N]_0$. Separate experiments were performed for determining the O^- rate constants, in which O^- was injected into the flow tube instead of O_2^-. Absolute uncertainties in the rate constants are on the order of ±40% and relative rate constants have uncertainties of ±25%. These are larger than the uncertainties normally reported for SIFT measurements of ±25% and ±15%, respectively. The larger error comes from more scatter in the data and the potential for atom loss on the flow tube walls. The latter effect cannot be measured so we treat these errors as estimates only. Relative errors (from one temperature to the next) are smaller since many of the errors are the same. Each reported rate constant is the average of about four runs.

Table I lists the present results along with literature values of the rate constants for 300 K. In general, all values are in good agreement. The present results are about 25% lower than those of Fehsenfeld *et al.*[2] with the exception of the O_2^- with O reaction. In this case the two values disagree by a factor of 1.9, which still is within the combined experimental error. Our agreement with the previous value from our laboratory (Poutsma *et al.*[6]) for the O_2^- with N reaction is similarly good, although in the opposite direction. However, the

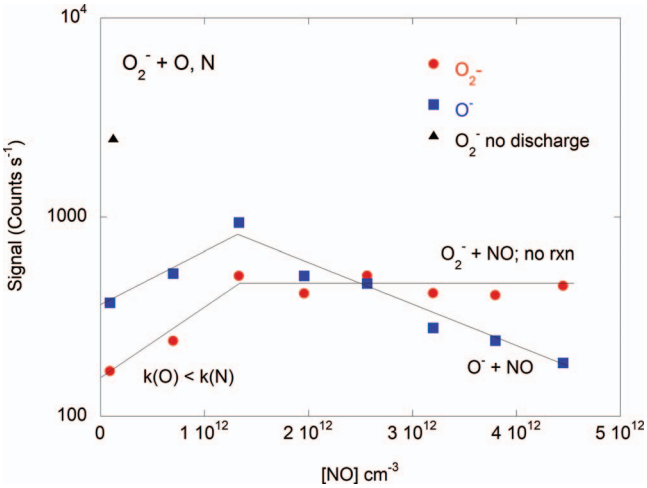

FIG. 1. O_2^- and O^- ion signals as a function of NO flow at 300 K and 0.8 Torr after a reaction time of 5.8 ms. The black triangle denotes data taken before the discharge was turned on.

TABLE I. Comparison of the reaction rate constants for reactions (1)–(4) measured at 300 K in units of 10^{-10} cm^3 s^{-1}. The last column is the temperature dependence measured in the current study (expressed as fits to a power law).

Reaction	Present	Poutsma *et al.*[6]	Fehsenfeld *et al.*[2]	n in T^{-n}
$O_2^- + N$	3.1	2.3	4.0	1.7 ± 0.3
$O_2^- + O$	1.7	3.9	3.3	1.8 ± 0.3
$O^- + N$	1.7		2.2	0.6 ± 0.3
$O^- + O$	1.5		1.9	1.3 ± 0.3

present O_2^- with O rate constant is over a factor of two lower than our previously reported value. While the two previous values for O_2^- with O (i.e., Poutsma *et al.* and Fehsenfeld *et al.*) appear to be in good agreement with each other, they have an opposite ordering of the N and O reactions, indicating the difficulty of the measurements. We speculate that our current value is more accurate for several reasons. Looking at the raw data figures (see Fig. 1 in both papers) shows a leveling out at high NO flows in the current study as expected, since NO does not react with O_2^-, while the previous study shows a slight decrease in the O_2^- signal after the titration end point. This indicates that the previous experiment had some signal drift as O atoms were added, presumably due to surface oxidation causing non-conducting layers. In the past, we were not able to measure temperature dependences for this reaction, because signal drift was worse than in our current setup, particularly above and below room temperature. A key difference between the instrument as employed in our previous study (at Hanscom AFB) and that at present is that all vacuum pumps have been replaced with oil-free pumps; a cleaner system may explain the difference.

Figure 2 shows the temperature dependences of the four reactions. Reactions were studied from 173 K to 400 K for O_2^- and 173 K to 500 K for O^-. The reduced upper temperature for the O_2^- reactions was due to the presence of thermal detachment for O_2^- at 500 K:[5]

$$O_2^- + He \rightarrow O_2 + e^- + He \quad \Delta_r H^\circ = 0.448\,eV. \qquad (6)$$

Evidence for reaction (6) is presented below. All data show a clear trend that increasing temperature decreases rate constants, as is often the case for ion-molecule reactions.[14,15] The fits shown in Fig. 2 are power laws and the exponents are listed in Table I. Both O_2^- reactions have similar temperature dependences, $T^{-1.7}$ and $T^{-1.8}$ for the N and O reactions, respectively. The O^- reactions have smaller temperature dependences, $T^{-0.6}$ and $T^{-1.3}$ for the N and O reactions, respectively. The smaller values for O^- reactions are expected since the reactants have no internal degrees of freedom.

Branching ratios for the reaction of $O_2^- + N$ were obtained by monitoring the intensity of both the O_2^- reactant and O^- product as a function of extent of reaction. The N concentration was varied by changing either the microwave discharge power or the N_2 flow. Figure 3 shows the raw data where the y-axis is the O^- count increase divided by the O_2^- count decrease (the O_2^- decrease is equal to the sum of all products produced). The x-axis is the extent of reaction, $\ln \frac{[O_2^-]_{off}}{[O_2^-]_{on}}$, where $[O_2^-]_{off}$ is the signal with the discharge off. There is a decline in the O^- fraction with increasing extent of reaction due to reaction (3). A linear least squares fit indicates 100% (from the y-intercept at 110%) branching to produce O^- (reaction (1b)). Looking at the graph we can give a lower limit of 85% O^- production. Previously, we have reported this as only 35%.[6] The difference should only be due to mass discrimination. In between the two experiments we upgraded our quadrupole control electronics so that a much higher frequency supply is now available for experiments in this mass range, 2.1 MHz vs. 1.2 MHz. We measured mass discrimination in the current study by studying the reaction of O^+ with O_2 producing O_2^+, i.e., the same masses. Discrimination was found to be less than 6%. Obviously, the same test cannot be done for the old measurements, but discrimination at low masses was sometimes a problem with the lower frequency electronics, though the extent of it appears to have been missed in this case because the O^- product also detaches electrons. At temperatures of 400 K and below we found that within our uncertainty (~20%), only O^- is produced, i.e.,

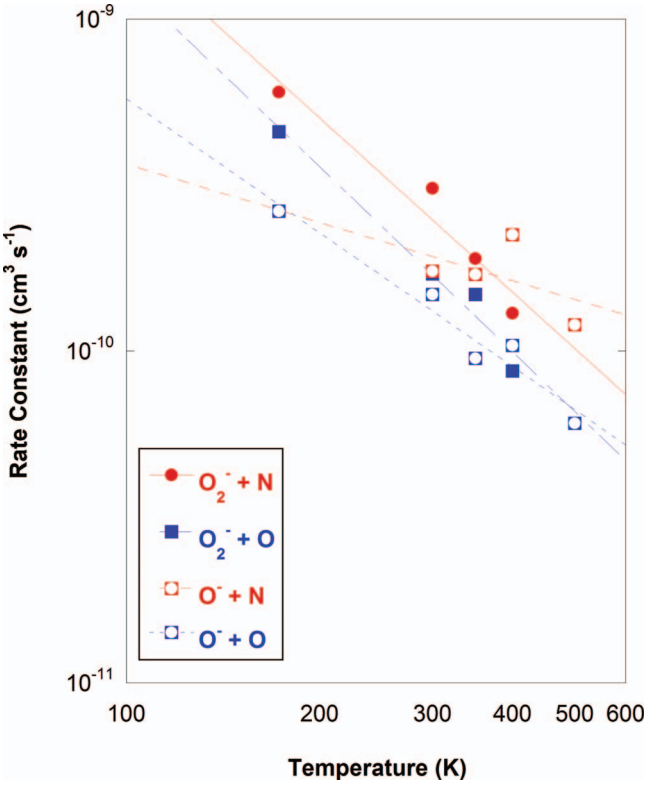

FIG. 2. Rate constants for the reactions of O_2^- and O^- with N and O as a function of temperature.

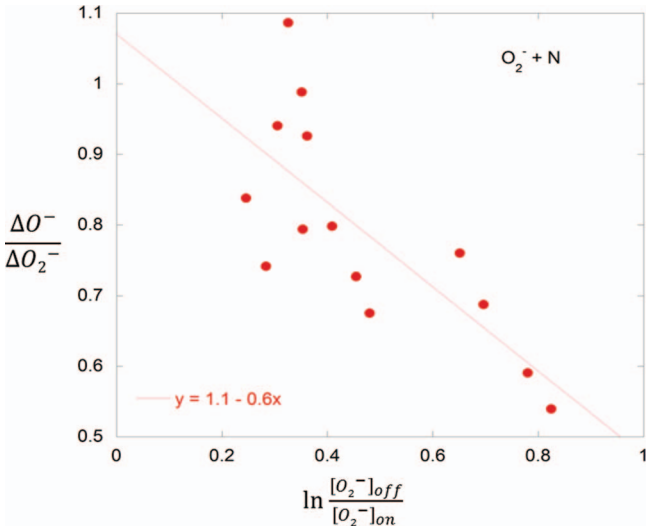

FIG. 3. Data used to derive branching for reaction (1). The y-axis is the amount of O^- increase divided by the O_2^- decrease ($\frac{\Delta O^-}{\Delta O_2^-}$) and the x-axis is the extent of reaction $\ln \frac{[O_2^-]_{off}}{[O_2^-]_{on}}$.

reaction (1b) dominates reaction (1b). At 500 K, we measured more O^- produced than O_2^- declined. We attribute that to the presence of reaction (6), i.e., the N atoms reacted with some of the O_2^- before it detached. Modeling the kinetics confirms this possibility but deriving accurate rate constants for reaction (6) is not possible. The branching ratios for reaction of $O_2^- + O$ were not determined in the present work due to both the presence of either N atoms or NO along with the O atoms, as well as secondary chemistry greatly complicating the analysis and preventing any meaningful results.

These measurements have direct relevance to mesospheric chemistry. Both O^- and O_2^- are found in appreciable abundance, as well as O atoms and to a lesser extent N atoms.[3,16–18] Since electrons interact with radio waves much more extensively than ions, processes that convert ions to electrons are important for communications. Our finding that N atoms do not directly produce electrons in reaction (1), but instead indirectly since the O^- produced reacts by detaching an electron, will not have a major effect since the N atom concentration in the mesosphere is much lower than that of O. What will have a larger effect is that the rate constants are all larger at low temperature and the mesosphere is typically cold, which should shift ions to electrons more rapidly. Insight into reactions (2)–(4) is difficult, as these reactions are challenging to model. The atom reactions involve electron reactions, cannot be modeled statistically, and are highly sensitive to details of the potential energy surfaces. The O_2^- reaction with O is charge transfer producing O_2, which is notoriously difficult to model properly.[19] More tractable theoretically is reaction (1), for which we have calculated the potential energy surface. The electronic state responsible for the reaction was found to be the lowest triplet ($1^3A''$) state. There have been very few *ab initio* studies of the NO_2 anion on this triplet state and the existing studies[20,21] only focused on the equilibrium geometry and energy without addressing the $N(^4S) + O_2^-(X^2\Pi_g)$ reaction. As a result, the reaction pathway leading to the formation of NO_2^- is surveyed here using several different theoretical methods. Two minima, both with C_{2v} symmetry, have been located at several different levels of theory, and their geometries, energies, and vibrational frequencies are summarized in Fig. 4. The global minimum features a larger O–N–O bond angle than the higher local minimum, and there exists an isomerization barrier between the two, which is not determined here. The situation here is quite similar to $O_3(1^3A'')$,[22] which is isoelectronic to $NO_2^-(1^3A'')$. Density functional theory (DFT) calculations with two different functionals (MPW1K[23] and ωB97X-D[24]) give similar results, while the spin-unrestricted explicitly correlated coupled cluster with singles, doubles, and perturbative triples calculations (UCCSD(T)-F12)[25] reduce the depth of the two minima slightly. These calculations used the augmented correlation-consistent polarized triple-zeta (AVTZ) basis set.[26] The UCCSD(T) and DFT calculations were performed with MOLPRO[27] and GAUSSIAN 09.[28]

Unfortunately, single reference approaches do not converge well in the reactant asymptote and other regions. The three-dimensional potential energy surface mapped at the DFT level is quite bumpy, making it difficult to identify the reaction pathway. The difficulties associated with the electronic

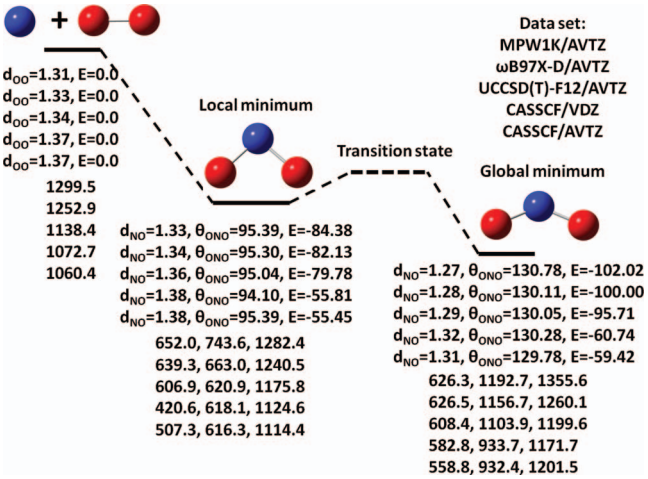

FIG. 4. Stationary points on the NO_2^- anion ($1^3A''$ state) potential energy surface, determined by various theoretical methods, as indicated in the upper right corner. The two minima are both in C_{2v} symmetry, and the corresponding bond lengths and bond angles are given in angstroms and degrees, respectively. Energies are listed in kcal/mol, while frequencies are given in cm^{-1}. Blue and red balls represent N and O atoms, respectively. The vibrational frequencies are listed in increasing order.

structure calculations are presumably due to the fact that there are many low-lying electronic states in the dissociation asymptote, even near the equilibrium, as was found for the O_3 molecule.[22] As a result, a multi-reference method, namely, the complete active space self-consistent field (CASSCF) method[29] implemented in MOLPRO[27] was used. It was noted that the valence active space typically failed to converge, but the inclusion of the 3*s* orbitals of the O atoms was found to improve convergence. In order to reduce the computational costs, the 1*s* and 2*s* orbitals of N and O were all treated as doubly occupied but the molecular orbital coefficients were fully optimized. The resulting active space of (11o, 12e) yielded 49104 configuration state functions. In addition, state-averaged CASSCF wave functions which include the two lowest A″ states with equal weights were employed.

As shown in Fig. 4, the optimized minima at the CASSCF level have similar geometries as those obtained from other methods, but have much smaller well depths relative to the $O_2^- + N$ reactant asymptote. This is apparently due to the neglect of dynamical correlation energy in the CASSCF method. Convergence remains an issue in the CASSCF calculations in the dissociation asymptote. After many attempts, we obtained a reaction path along the Jacobi coordinate *R*, which is the distance between N and the center of mass of O_2^-, with other degrees of freedom relaxed, employing the relatively small VDZ basis set. As shown in Fig. 5, it has a small barrier ($d_{NO} = 1.9$ Å, $d_{OO'} = 1.36$ Å, $\theta_{ONO'} = 116°$) about 0.6 kcal/mol above the reactants. It is interesting, however, the barrier disappears at the complete active space second-order perturbation (denoted as CASPT2 in MOLPRO) level,[30] which captures part of dynamical correlation. It should be noted that the total number of contracted configuration state functions reached 84 687 237 in the CASPT2, making the computations extremely time-consuming. Consequently, higher levels of *ab initio* methods, such as the multi-reference configuration

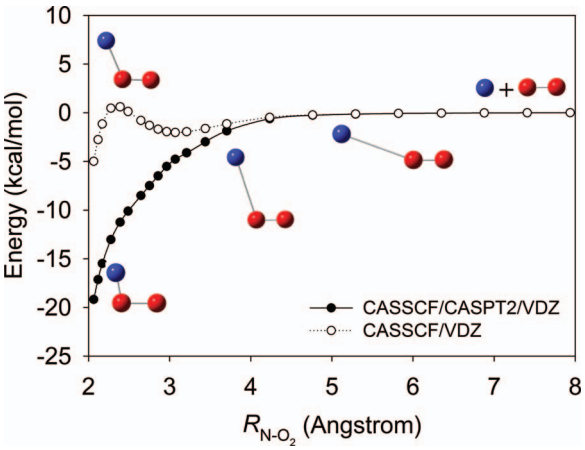

FIG. 5. Potential energy curves as a function of N–O_2^- Jacobi distance with other coordinates optimized at the CASSCF/VDZ level. The open and solid circles correspond to the CASSCF and CASPT2 energies, respectively, at the CASSCF optimized geometries.

interaction (MRCI) calculations, are not presently feasible for this molecule due to formidable computational costs.

The negative temperature dependence of the rate constant suggests a barrierless reaction pathway. Indeed, the CASPT2 curve presents no barrier, consistent with the experimental data and demonstrates the importance of dynamical correlation energy in this system. The situation here is similar to the case of O + O_2 where a similar entrance channel barrier has been shown to disappear when progressively larger basis sets and higher-level *ab initio* methods are used.[31] A more reliable determination of the entrance channel potential energy surface would require a larger basis set and an even higher level of *ab initio* treatment. Such calculations are still extremely challenging.

The observation of O_2^- + N producing primarily NO and O^-, approaching 100%, as opposed to NO_2 + e^- deserves comment, as the latter channel is 1.72 eV more exothermic than the former. This is potentially due to the behavior of the specific rate curves for detachment and dissociation from NO_2^-. As seen in the case of SF_6^-[32] (typical of barrierless, highly exothermic cases such as this), the rate constant for dissociation scales much more sharply with respect to energy than does that for detachment, with a larger asymptotic value as well (see Fig. 5 in Ref. 32). This is due to the larger number of contributing states in the case of dissociation, since detachment is usually s-wave, reducing the number of potential rotational states that can conserve orbital angular momentum. To test the applicability an approach similar to that employed in Ref. 32 has been attempted for the current system, calculating the specific rate curve for dissociation of J = 0 NO_2^{-*} to O^- + NO using Orbiting Transition State–Phase Space Theory and that of electron detachment via microscopic reversibility by fitting to experimental data of thermal associative electron attachment to NO_2. At the energy of the reactants, the ratio of the resulting calculated number of states for dissociation to that of detachment is 20:1, suggesting a branching of >95%, consistent with our experimental results. However, the calculated absolute rate constants approach 10^{14} s^{-1}, a timescale competitive with that of intramolecular vibrational energy redistribution, suggesting that a statistical approach may not be appropriate. As such, a quantitative description of the reaction appears to require a complete PES description, which is not currently available, and we are limited to the above qualitative discussion of the branching.

CONCLUSIONS

In conclusion, we have reported the rate constants for the reactions of O^- and O_2^- with N and O atoms from 173 to 500 K for the reactions with O^- and 173-400 K for the reactions with O_2^- for the first time. The room temperature values agreed reasonably well with previous measurements, with the exception of the reaction of O_2^- + O. The discrepancy in this case is likely due to the absence of significant signal drift arising from surface oxidation instilling insulating layers, an effect minimized due to the oil-free nature of the current system. Additionally, in contrast to previous reports, we have found the O_2^- + N reacts to form predominantly (>85%) NO + O^-, at all temperatures where a branching determination was available. We attribute this to specific rate curves for detachment rising more slowly with energy than for dissociation. Importantly, all of the studied reactions were found to display negative temperature dependences, increasing their importance in mesospheric chemistry, where the lower temperatures ensure that these reactions will be occurring faster than the previously reported room temperature rates.

ACKNOWLEDGMENTS

We are grateful for the support of the Air Force Office of Scientific Research for this work under Project No. AFOSR-2303EP. J.J.M. and S.G.A. acknowledge the support of the National Research Council. H.G. acknowledges financial support from Department of Energy (DOE) (DE-FG02-05ER15694).

[1] A. Dalgarno, Ann. Geophys. **17**, 16 (1961).
[2] F. C. Fehsenfeld, A. L. Schmeltekopf, H. I. Schiff, and E. E. Ferguson, Planet. Space Sci. **15**, 373 (1967).
[3] E. E. Ferguson, F. C. Fehsenfeld, and D. L. Albritton, in *Gas Phase Ion Chemistry*, edited by M. T. Bowers (Academic, San Diego, 1979), Vol. 1, pp. 45–82.
[4] A. S. Jursa, *Handbook of Geophysics and the Space Environment* (National Technical Information Service, Springfield, VA, 1985).
[5] P. J. Linstrom and W. G. Mallard, Eds., NIST Chemistry WebBook, NIST Standard Reference database Number 69, (National Institutes of Standards and Technology, Gaithersburg, MD, 2005), (http://webbook.nist.gov).
[6] J. C. Poutsma, A. J. Midey, and A. A. Viggiano, J. Chem. Phys. **124**, 074301 (2006).
[7] A. A. Viggiano, Phys. Chem. Chem. Phys. **8**, 2557–2571 (2006).
[8] A. A. Viggiano, R. A. Morris, F. Dale, J. F. Paulson, K. Giles, D. Smith, and T. Su, J. Chem. Phys. **93**, 1149–1157 (1990).
[9] A. A. Viggiano and R. A. Morris, J. Phys. Chem. **100**, 19227–19240 (1996).
[10] A. A. Viggiano, R. A. Morris, and J. F. Paulson, Int. J. Mass Spectrom. Ion Process. **135**, 31–37 (1994).
[11] A. A. Viggiano, F. Howorka, D. L. Albritton, F. C. Fehsenfeld, N. G. Adams, and D. Smith, Astrophys. J. **236**, 492 (1980).
[12] A. L. Schmeltekopf, E. E. Ferguson, and F. C. Fehsenfeld, J. Chem. Phys. **48**(7), 2966 (1968).
[13] F. Kaufman, Prog. React. Kinet. **1**, 1–39 (1961).
[14] Y. Ikezoe, S. Matsuoka, M. Takebe, and A. Viggiano, *Gas Phase Ion-Molecule Reaction Rate Constants through 1986* (Ion Reactions Research Group of The Mass Spectrometry Society of Japan, Tokyo, 1987).

[15]V. Anicich, Report No. JPL 03-19, 2003.
[16]M. C. Kelly, *The Earth's Ionosphere* (Academic Press, San Diego, CA, 1989).
[17]F. Arnold, J. Kessel, D. Krankowsky, H. Wieder, and J. Zahringer, J. Atmos. Terr. Phys. **33**, 1169–1175 (1971).
[18]G. P. Brasseur and S. Solomon, *Aeronomy of the Middle Atmosphere* (Springer, Dordrecht, 2005).
[19]G. Schatz, personal communication (2013).
[20]Z. L. Cai, J. Chem. Soc., Faraday Trans. **89**(7), 991–994 (1993).
[21]J. Czernek and O. Živný, Chem. Phys. Lett. **435**(1–3), 29–33 (2007).
[22]H. Han, B. Suo, D. Xie, Y. Lei, Y. Wang, and Z. Wen, Phys. Chem. Chem. Phys. **13**, 2723–2731 (2011).
[23]B. J. Lynch, P. L. Fast, M. Harris, and D. G. Truhlar, J. Phys. Chem. A **104**, 4811–4815 (2000).
[24]J.-D. Chai and M. Head-Gordon, Phys. Chem. Chem. Phys. **10**, 6615–6620 (2008).
[25]T. B. Adler, G. Knizia, and H.-J. Werner, J. Chem. Phys. **127**, 221106 (2007).
[26]A. K. Wilson, D. E. Woon, K. A. Peterson, and J. T. H. Dunning, J. Chem. Phys. **110**(16), 7667–7676 (1999).
[27]H.-J. Werner, P. J. Knowles, G. Knizia *et al.*, MOLPRO, version 2010.1, 2010, a package of *ab initio* programs.
[28]M. J. Frisch, G. W. Trucks, H. B. Schlegel *et al.*, GAUSSIAN 09, Revision A.01, Gaussian, Inc., Wallingford, CT, 2009.
[29]H.-J. Werner and P. J. Knowles, J. Chem. Phys. **82**, 5053 (1985).
[30]H. J. Werner, Mol. Phys. **89**(2), 645–661 (1996).
[31]R. Dawes, P. Lolur, J. Ma, and H. Guo, J. Chem. Phys. **135**, 081102 (2011).
[32]J. Troe, T. M. Miller, and A. A. Viggiano, J. Chem. Phys. **127**, 244304 (2007).

DISTRIBUTION LIST

DTIC/OCP
8725 John J. Kingman Rd, Suite 0944
Ft Belvoir, VA 22060-6218 1 cy

AFRL/RVIL
Kirtland AFB, NM 87117-5776 2 cys

Official Record Copy
AFRL/RVBXT/Dr. Albert Viggiano 1 cy